Electronic Supplementary Material (ESI) for Journal of Materials Chemistry C.
This journal is © The Royal Society of Chemistry 2022

Supporting Information

Hybrid lanthanide-doped rattle-type thermometers for theranostics

Hannes Rijckaert,[#] Sonali Mohanty,[#] Joost Verduijn, Mirijam Lederer, Brecht Laforce, Laszlo Vincze, Andre Skirtach, Kristof Van Hecke*, Anna M. Kaczmarek*

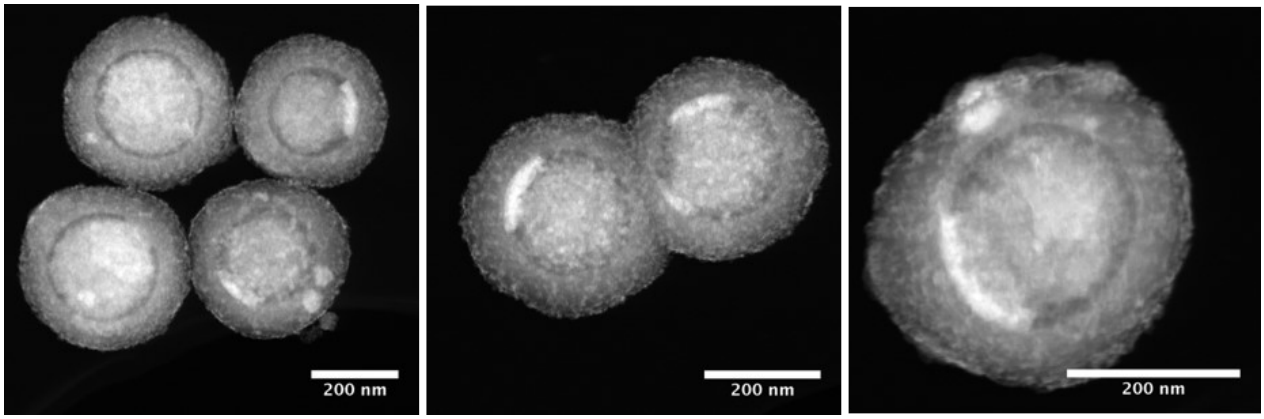

Figure S1. HAADF-STEM images of SiO_2@PMO material (before etching) with built in CaF_2:Er,Yb nanoparticles, synthesized at 0.3 M precursors, without the use of vacuum. As can be seen there are small voids in the SiO_2@PMO material between the SiO_2 and PMO where the CaF_2:Er,Yb,Tm builds in.

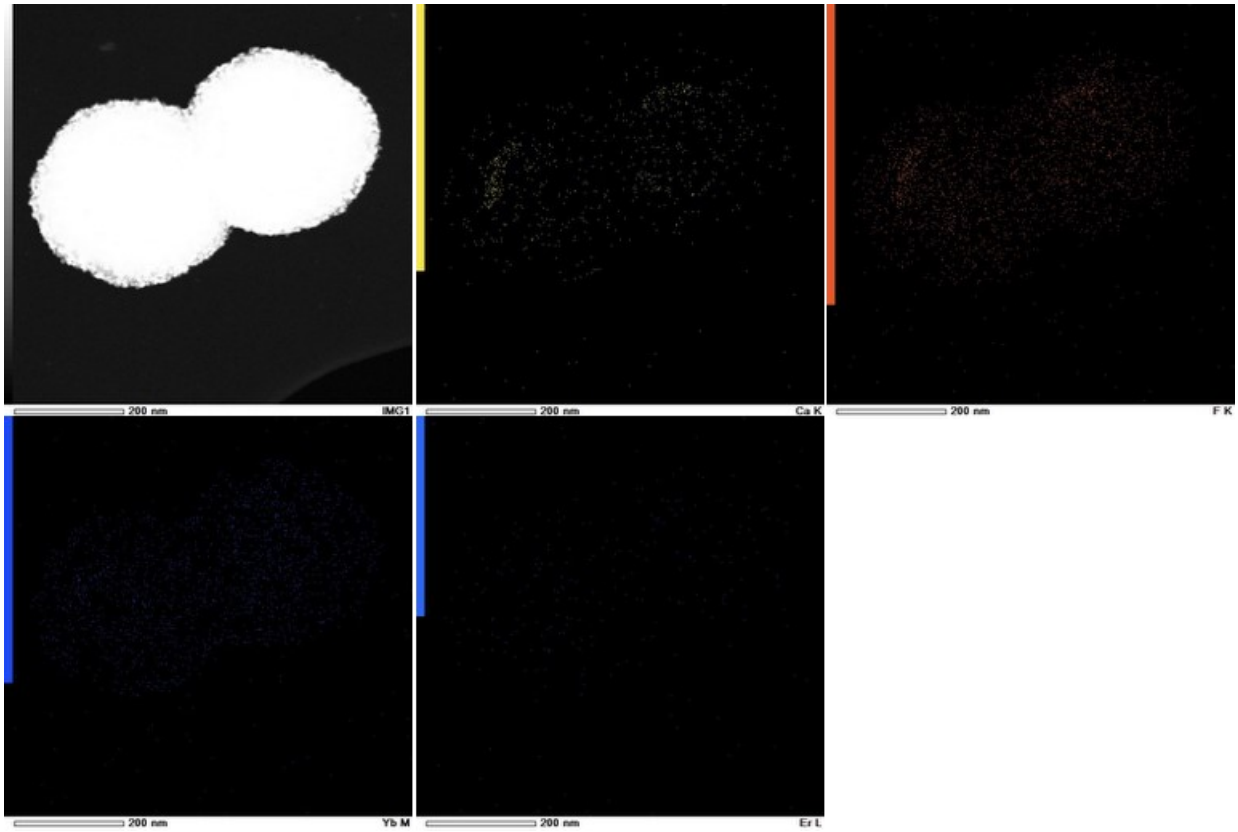

Figure S2. HAADF-STEM with EDX mapping of SiO_2@PMO:CaF_2:Er,Yb material. Ca, F, Y, Yb and Er were mapped. It can be seen that the CaF_2:Er,Yb,Tm builds in in the voids between SiO_2 and PMO as well as on the outer surface of the spherical particles.

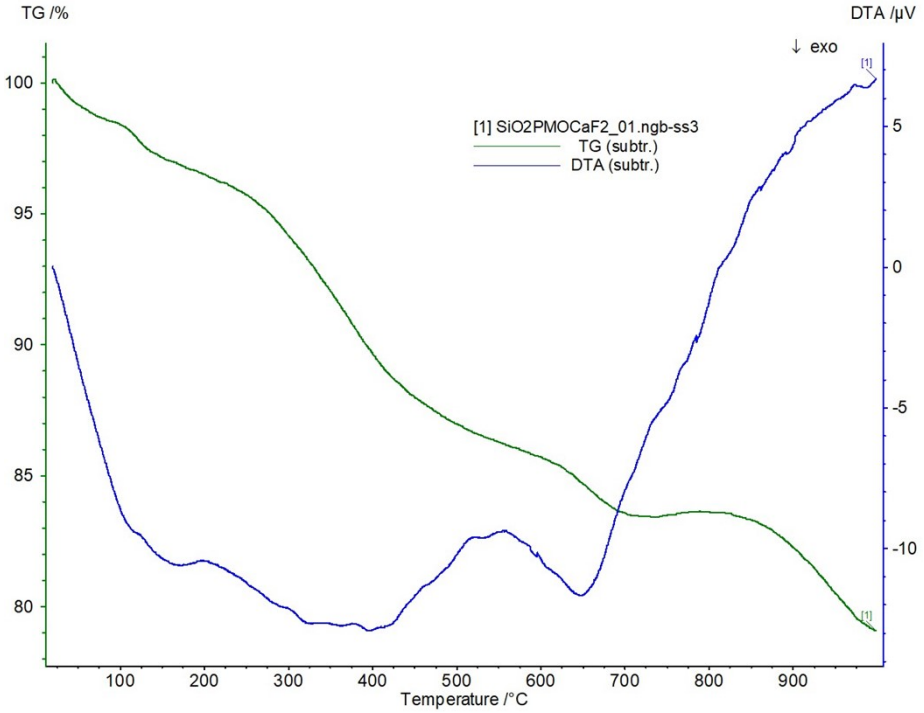

Figure S3. TGA of HPMO@CaF_2 material.

Table S1. Overview of the size distribution of the various PMO and HPMO spheres as well as $NaYF_4$ nanoparticles inside the hollow spheres (some discrepancy in the original size of the spheres is observed as sample HPMO@$NaYF_4$ vac 0.2 M was made from a new batch of material. Expansion of the spheres after SiO_2 removal was typically observed. Shrinkage of spheres was observed after filling with NP precursors and heat treatment (most likely shrinkage is a result of the additional heat treatment process).

	Spheres	**Hollow cavity**	**SiO_2 core**	**$NaYF_4$ NPs**
SiO_2@PMO (Fig. 1)	345.9±26.9 nm	-	193.5±19.2 nm	-
HPMO (Fig. 1)	392.0±26.4 nm	233.3±15.8 nm	-	-
HPMO@$NaYF_4$ no vac 0.3 M (Fig. 2)	331.3±17.7 nm	208.7±16.9 nm	-	41.3±16.8 nm
HPMO@$NaYF_4$ vac 0.1 M (Fig. 3)	302.3±21.1 nm	206.7±14.6 nm	-	29.1±5.7 nm
HPMO@$NaYF_4$ vac 0.2 M (Fig. 4)	401.1±31.4 nm	264.8±33.5 nm	-	99.6±40.0 nm
HPMO@$NaYF_4$ vac 0.3 M (Fig. 5)	301.9±28.9 nm	204.9±19.2 nm	-	58.4±21.2 nm

Table S2. Overview of the degree of loading HPMOs with $NaYF_4$ nanoparticles.

HPMO@$NaYF_4$ 0.3 M	No vac	10% loading
HPMO@$NaYF_4$ 0.1 M	Vac	18% loading
HPMO@$NaYF_4$ 0.2 M	Vac	32% loading
HPMO@$NaYF_4$ 0.3 M	Vac	41% loading

Table S3. Relative Ln^{3+} contents for the samples during synthesis (calcd.) and as determined by WDXRF. Large deviations are observed especially in the HPMO@CaF_2:Er,Yb,Tm materials. This can be linked to the difficult to control synthesis from precursors that partially build in. However, in the PXRD patterns of the HPMO@CaF_2:Er,Yb,Tm materials no additional phases besides the CaF_2 material are observed.

Sample	Yb^{3+} ion (%)		Er^{3+} ion (%)		Tm^{3+} ion (%)	
	Calcd.	WDXRF	Calcd.	WDXRF	Calcd.	WDXRF
HPMO@$NaYF_4$:Er,Yb	30	34.7	3	3.4	0	0
HPMO@$NaYF_4$:Er,Yb,2Tm	30	30.8	3	3.2	2	1.7
HPMO@$NaYF_4$:Er,Yb,4Tm	30	31.5	3	3.1	4	2.8
HPMO@$NaYF_4$:Er,Yb,6Tm	30	30.0	3	3.0	6	6.7
HPMO@$NaYF_4$:Er,Yb,8Tm	30	27.2	3	3.1	8	8.9
HPMO@$NaYF_4$:Er,Yb,10Tm	30	33.4	3	3.5	10	13.1
HPMO@CaF_2:Er,Yb	30	47.0	3	4.3	0	0
HPMO@CaF_2:Er,Yb,4Tm	30	51.0	3	6.7	4	7.2
HPMO@CaF_2:Er,Yb,6Tm	30	48.4	3	5.9	6	10.2
HPMO@CaF_2:Er,Yb,8Tm	30	37.7	3	4.5	8	9.4
Na_3ZrF_7:Er,Yb,0.5Tm	20	24.9	2	2.7	0.5	1.2

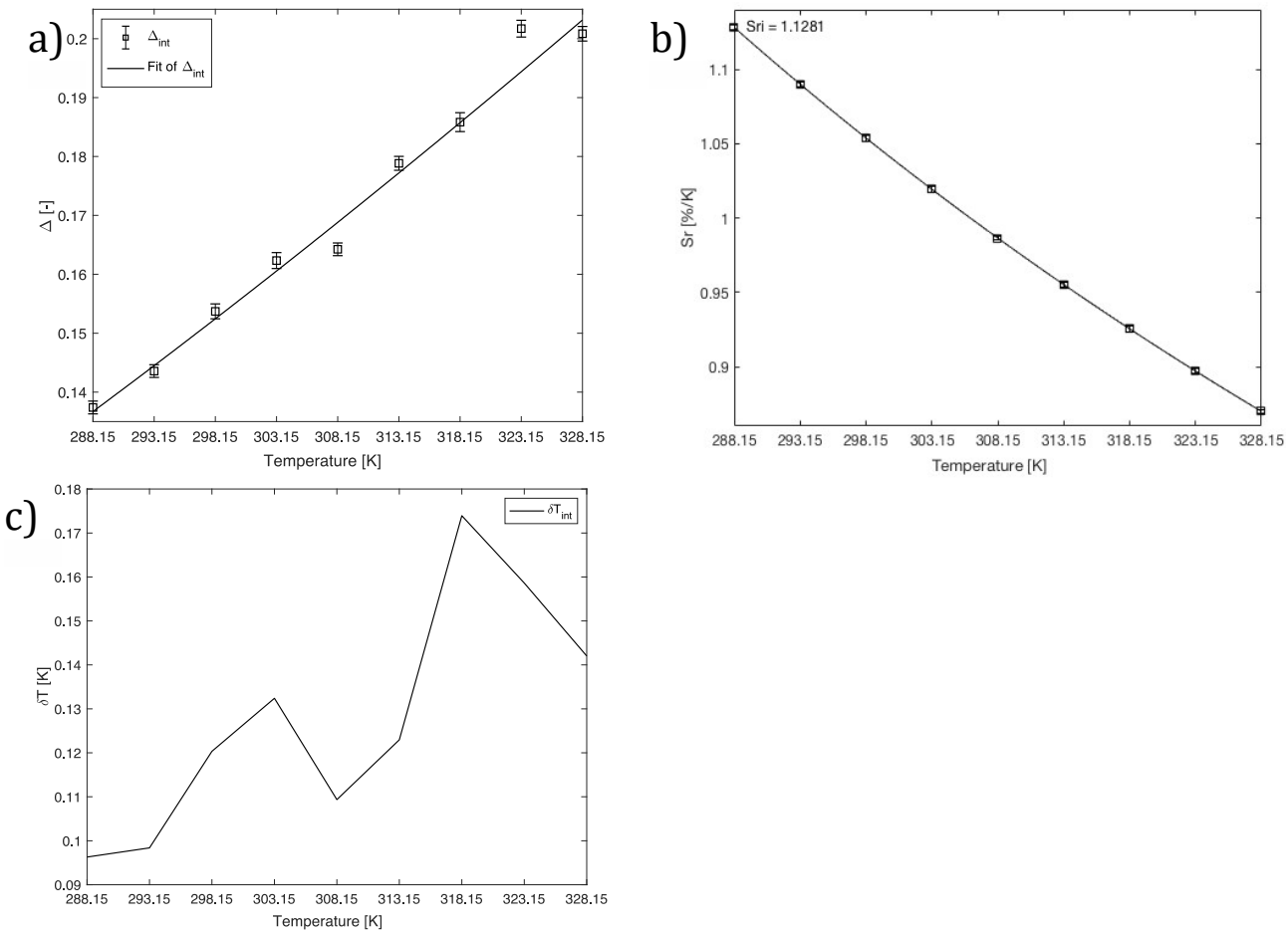

Figure S4. a) Plot showing the calibration curve for the HPMO@$NaYF_4$:Er,Yb material using eqn 2. The 520 nm and 540 nm peaks were used for calculations. The points show the experimental delta parameters, and the solid line shows the least squares fit to the experimental points. b) Plot of the relative sensitivity S_r at varying temperatures (288.15 – 328.15 K), the solid lines are a guide for the eyes. c) Graph depicting the temperature uncertainty over the regarded temperature range.

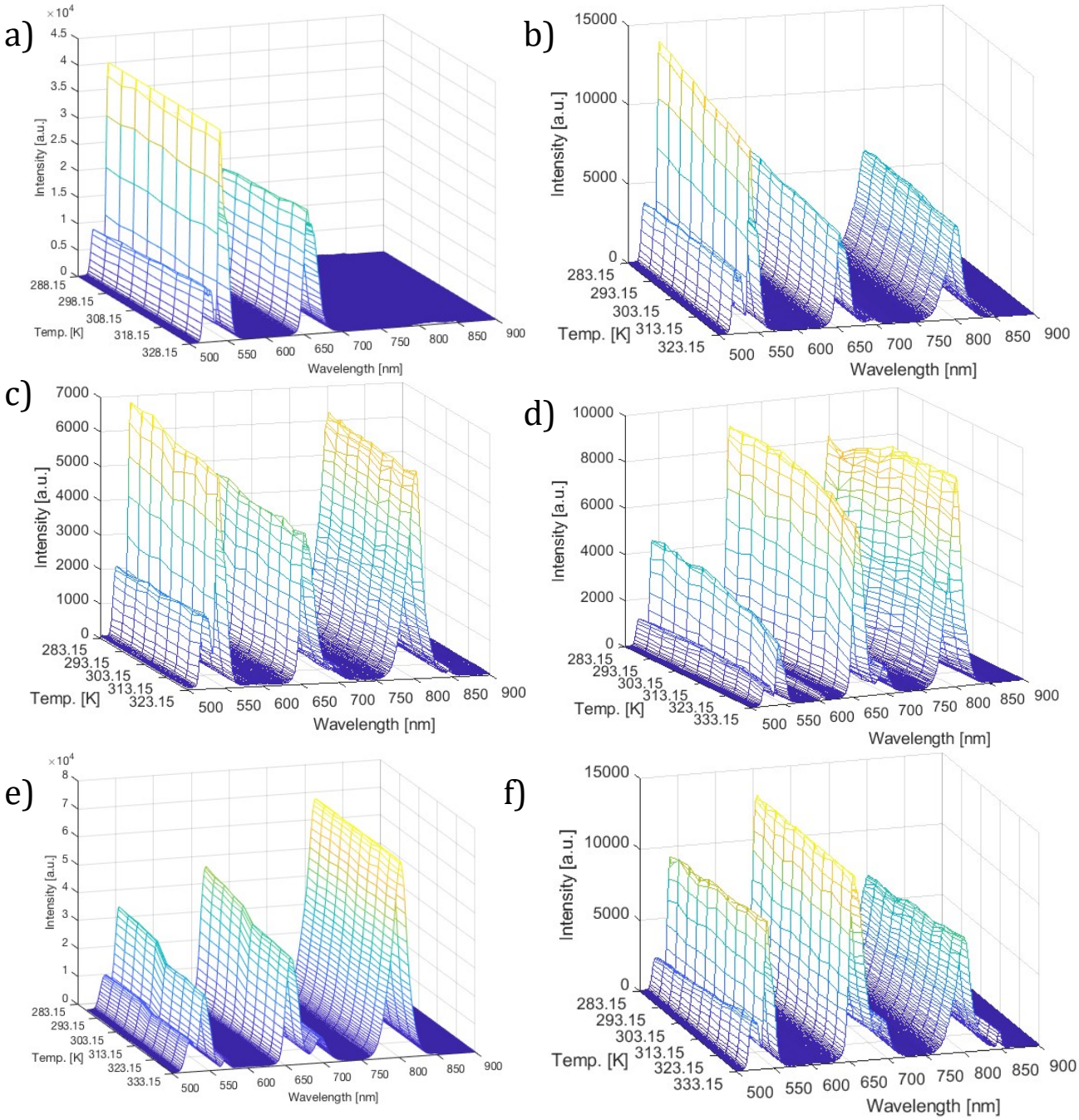

Figure S5. Emission maps of a) HPMO@$NaYF_4$:Er,Yb, b) HPMO@$NaYF_4$:Er,Yb,2Tm, c) HPMO@$NaYF_4$:Er,Yb,4Tm, d) HPMO@$NaYF_4$:Er,Yb,6Tm, e) HPMO@$NaYF_4$:Er,Yb,8Tm, and f) HPMO@$NaYF_4$:Er,Yb, 10Tm. The temperature range varied from 283.15 – 333.15 K.

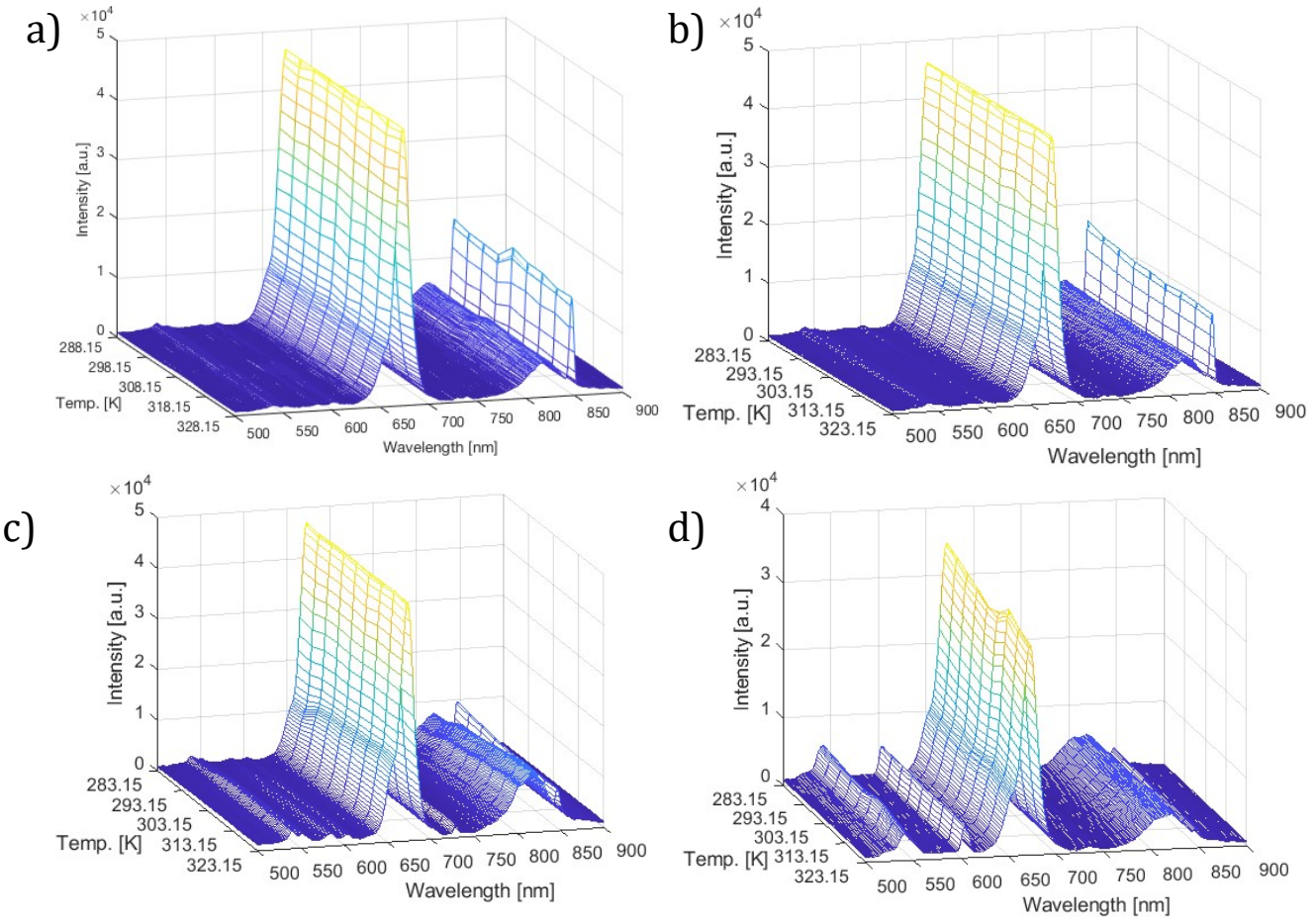

Figure S6. Emission maps of a) HPMO@CaF_2:Er,Yb, b) HPMO@CaF_2:Er,Yb,4Tm, c) HPMO@CaF_2:Er,Yb,6Tm, and d) HPMO@CaF_2:Er,Yb,8Tm. The temperature range varied from 283.15 – 328.15 K.

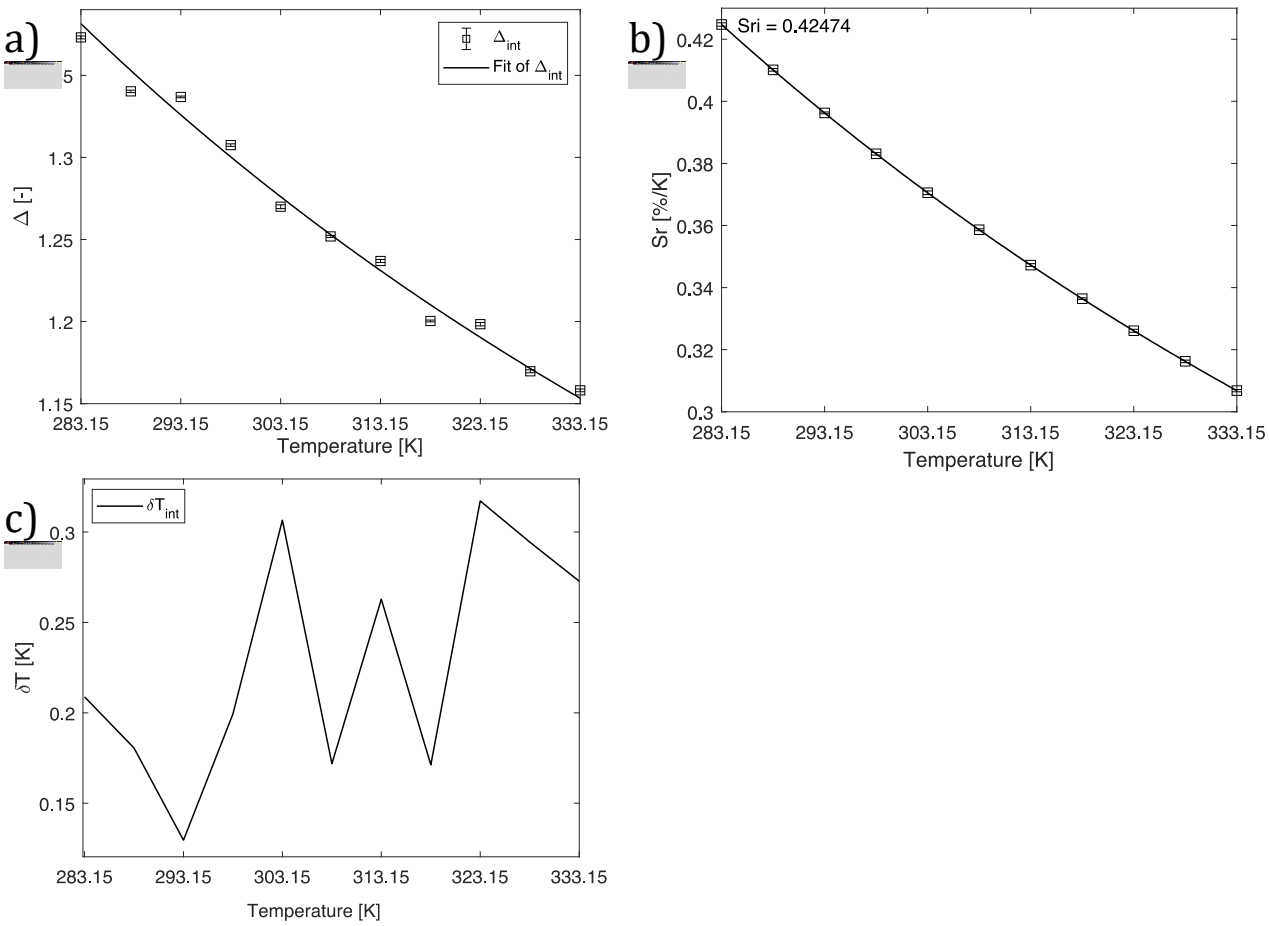

Figure S7. a) Plot showing the calibration curve for the HPMO@$NaYF_4$:Er,Yb,8Tm material using eqn 3. The points show the experimental delta parameters, and the solid line shows the least squares fit to the experimental points. b) Plot of the relative sensitivity S_r at varying temperatures (283.15 – 333.15 K), the solid lines are a guide for the eyes. c) Graph depicting the temperature uncertainty over the regarded temperature range.

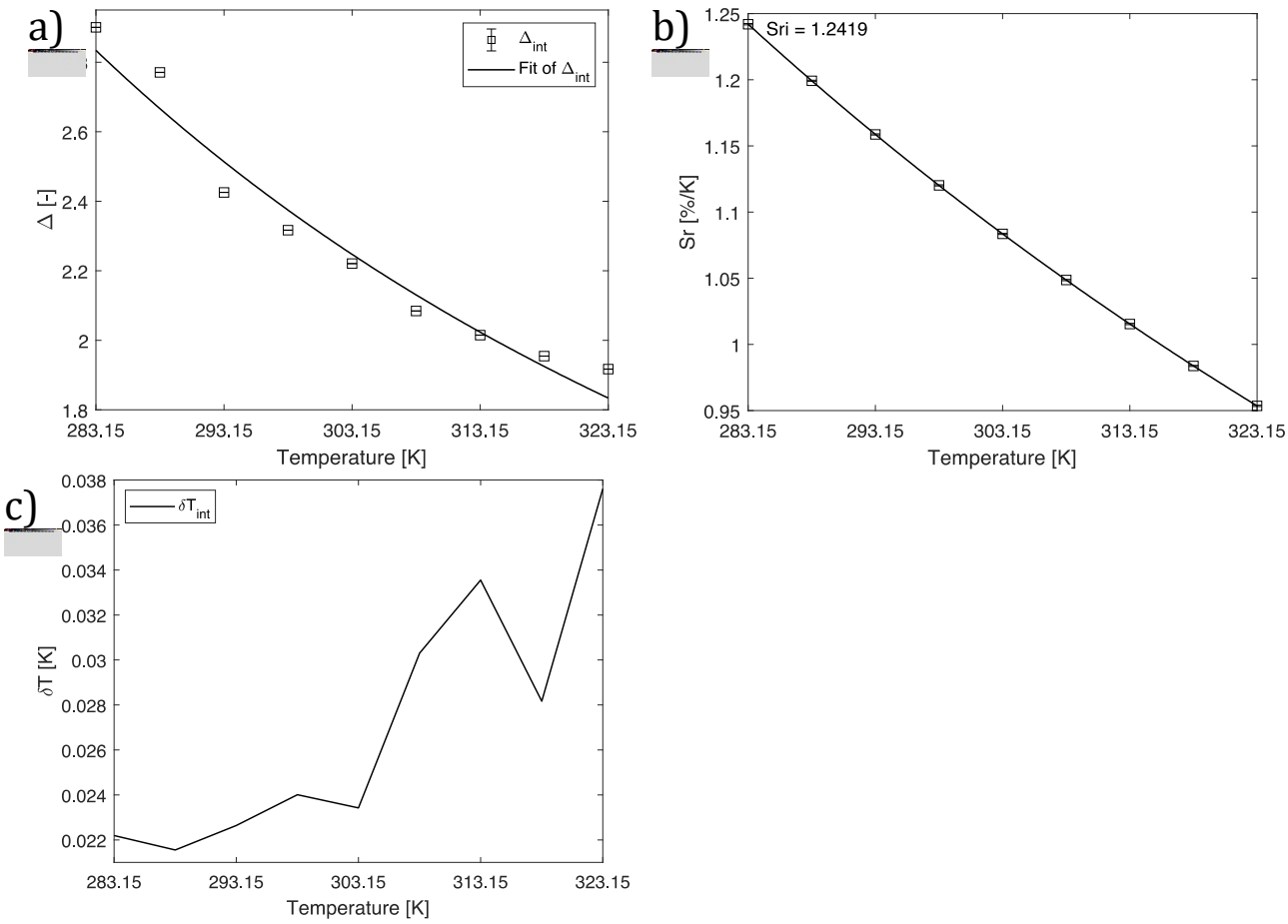

Figure S8. a) Plot showing the calibration curve for the HPMO@CaF_2:Er,Yb,6Tm material using eqn 3. The points show the experimental delta parameters and the solid line shows the least squares fit to the experimental points. b) Plot of the relative sensitivity S_r at varying temperatures (283.15 – 323.15 K), the solid lines are a guide for the eyes. c) Graph depicting the temperature uncertainty over the regarded temperature range.

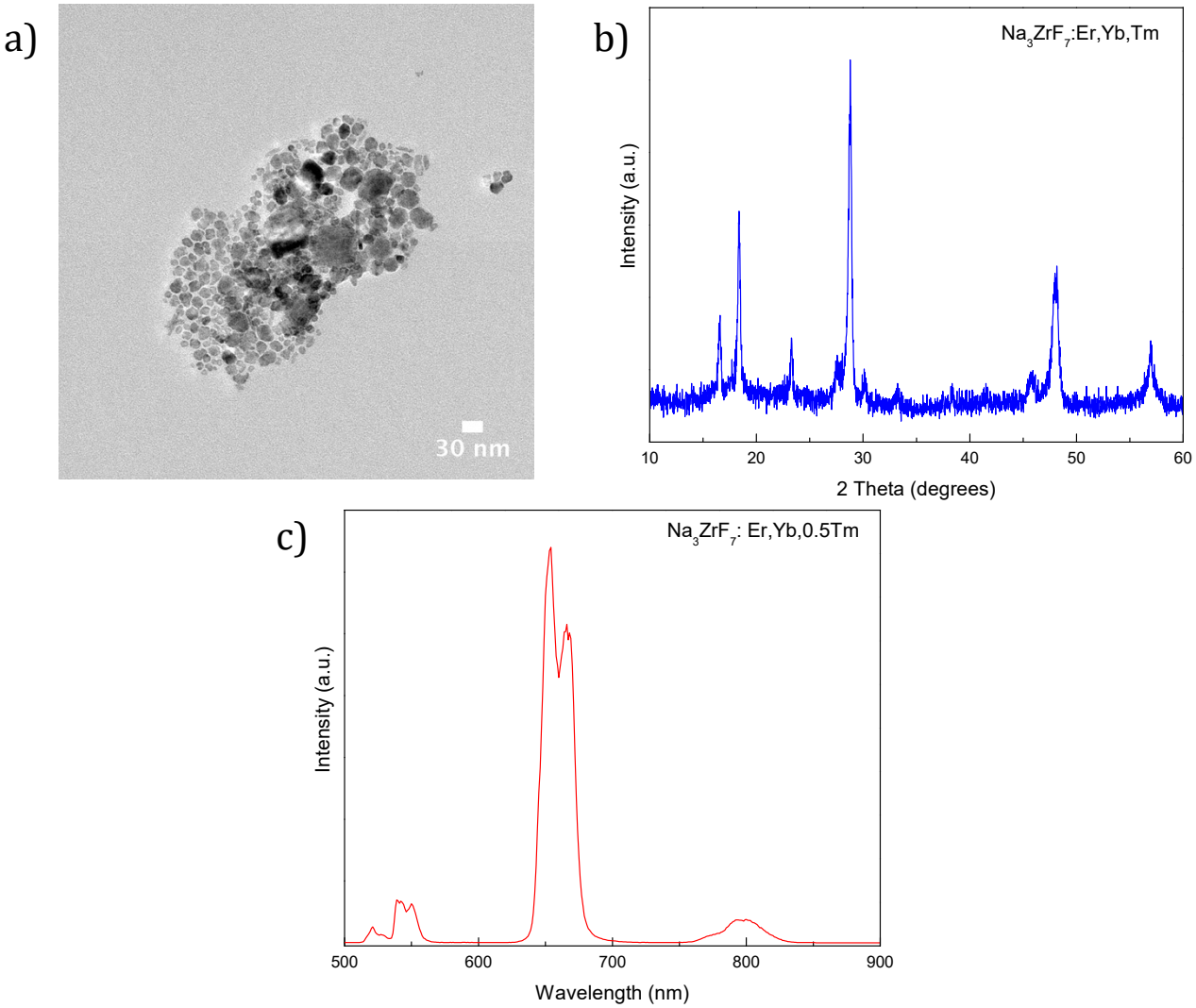

Figure S9. a) TEM image of Na_3ZrF_7:Er,Yb,0.5Tm nanoparticles prepared according to literature procedure[1], b) powder XRD diffractogram of the Na_3ZrF_7:Er,Yb,0.5Tm nanoparticles, c) RT emission spectrum of Na_3ZrF_7:Er,Yb,0.5Tm.

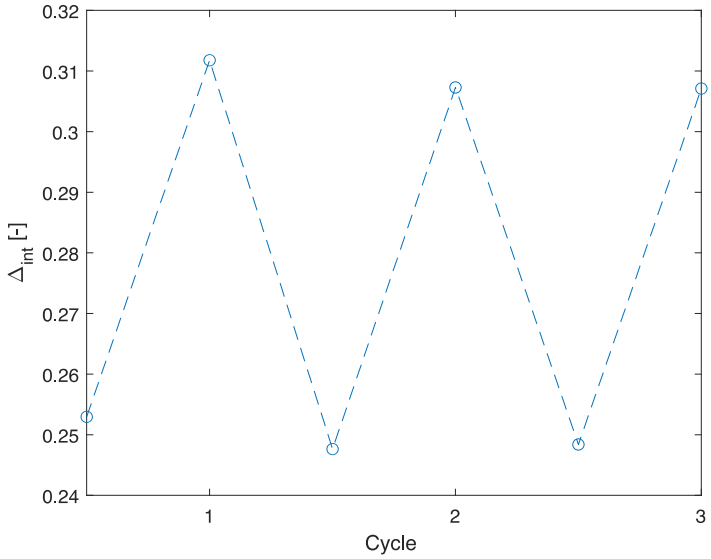

Figure S10. Cycle tests for carried out for HPMO@$NaYF_4$:Er,Yb material. A repeatability of 98% was observed.

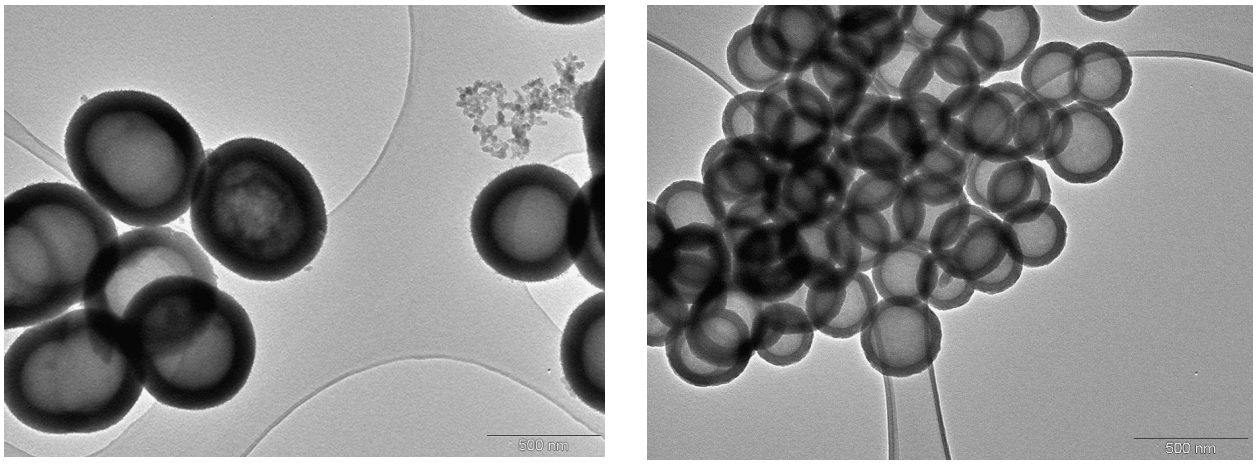

Figure S11. Left: TEM images of HPMO2 (ethane PMO) and right: HPMO3 (benzene and 3-aminopropyl)triethoxysilane PMO).

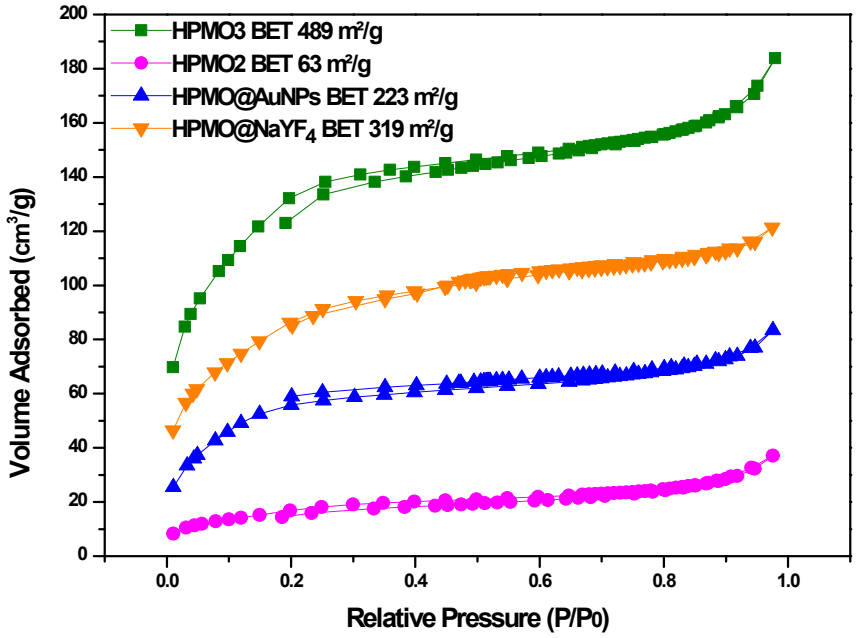

Figure S12. N_2 sorption for HPMO2, HPMO3, HPMO@AuNPs, and HPMO@$NaYF_4$. The presented here HPMO@$NaYF_4$ sample was prepared with 0.2 M precursors and was the sample used for DOX loading and release experiments.

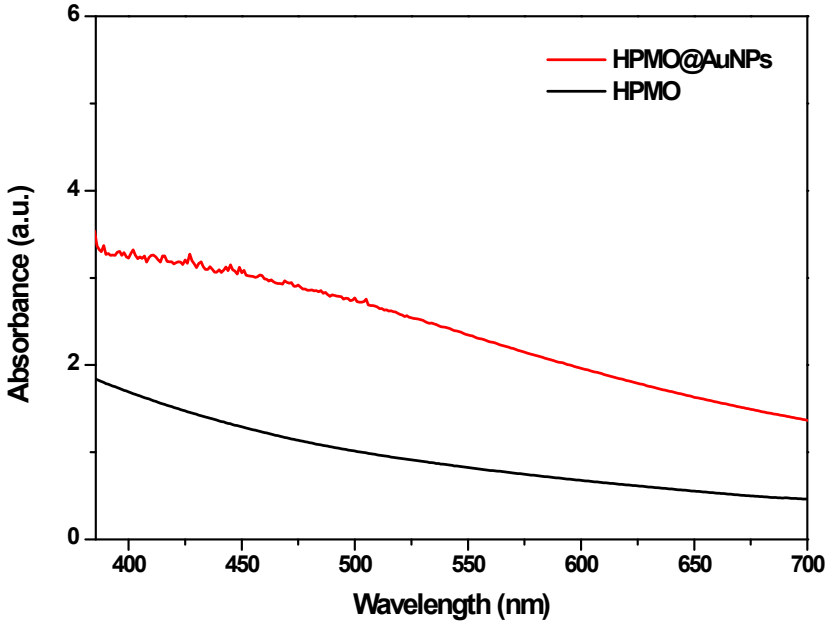

Figure S13. UV-Vis absorption spectrum of HPMO@AuNPs. The UV-Vis absorption spectrum of pristine HPMO is shown for comparison for clarity that no absorbance from the PMO itself is observed in this region.

DOX drug loading and release

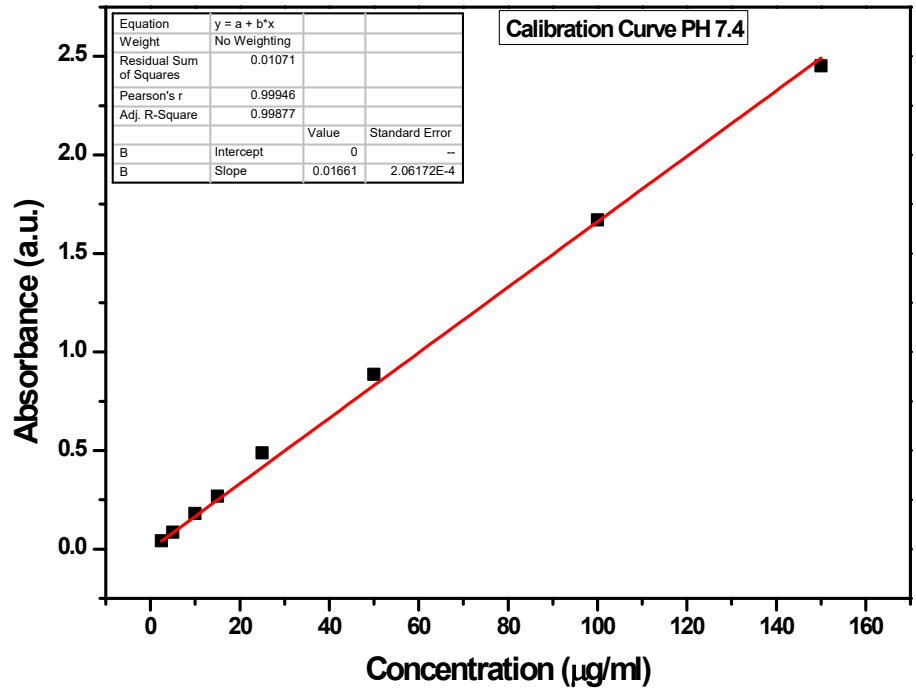

Figure S14. DOX calibration curve for PBS pH 7.4.

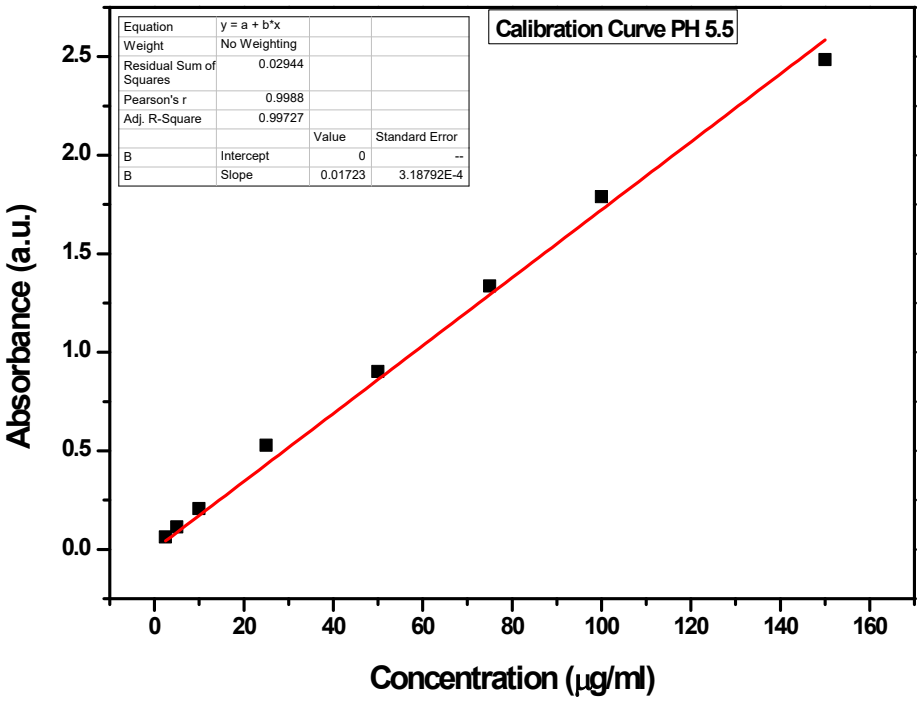

Figure S15. DOX calibration curve for PBS pH 5.5.

Table S4. Overview of the LC% and EE% values obtained for all investigated materials in this work.

Material	LC%	EE%
HPMO (pH = 7.4 T = 37 °C)	41.8	71.8
HPMO (pH = 5.5 T = 37 °C)	44.7	80
HPMO (pH = 5.5 T = 42 °C)	44.7	80
HPMO2 (pH = 5.5 T = 42 °C)	44.2	79.1
HPMO3 (pH = 5.5 T = 42 °C)	35.1	52
HPMO@AuNPs (pH = 5.5 T = 42 °C)	41.3	70.4
HPMO@$NaYF_4$ (pH = 5.5 T = 42 °C)	7.2	7.8

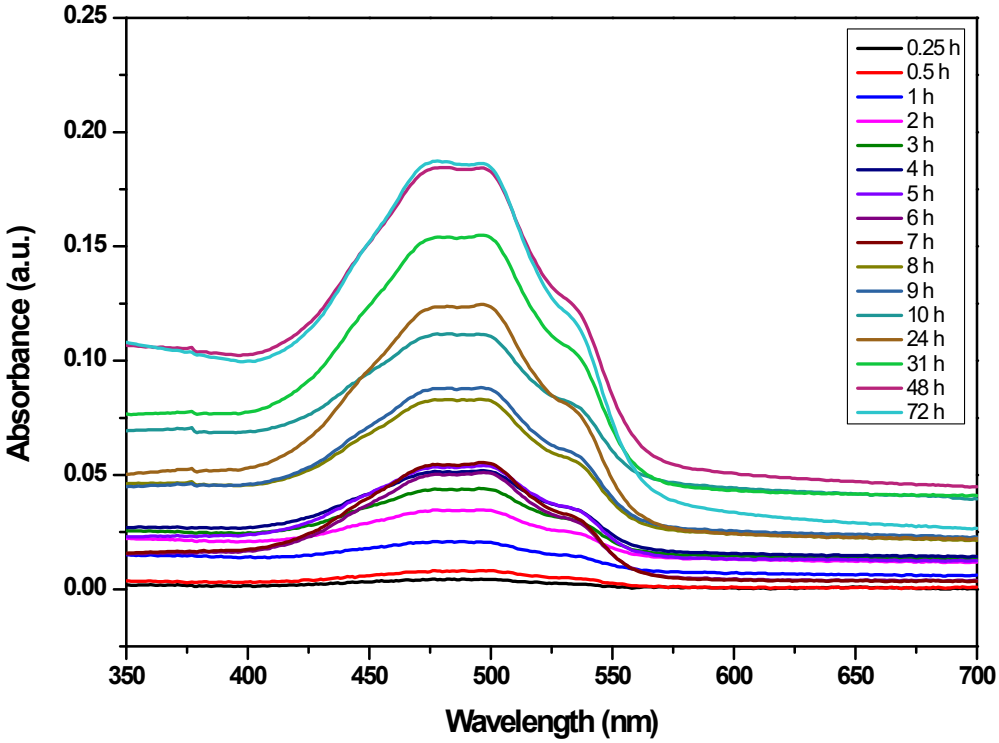

Figure S16. UV-Vis absorption spectra of DOX release form HPMO at pH 7.4 (37 °C).

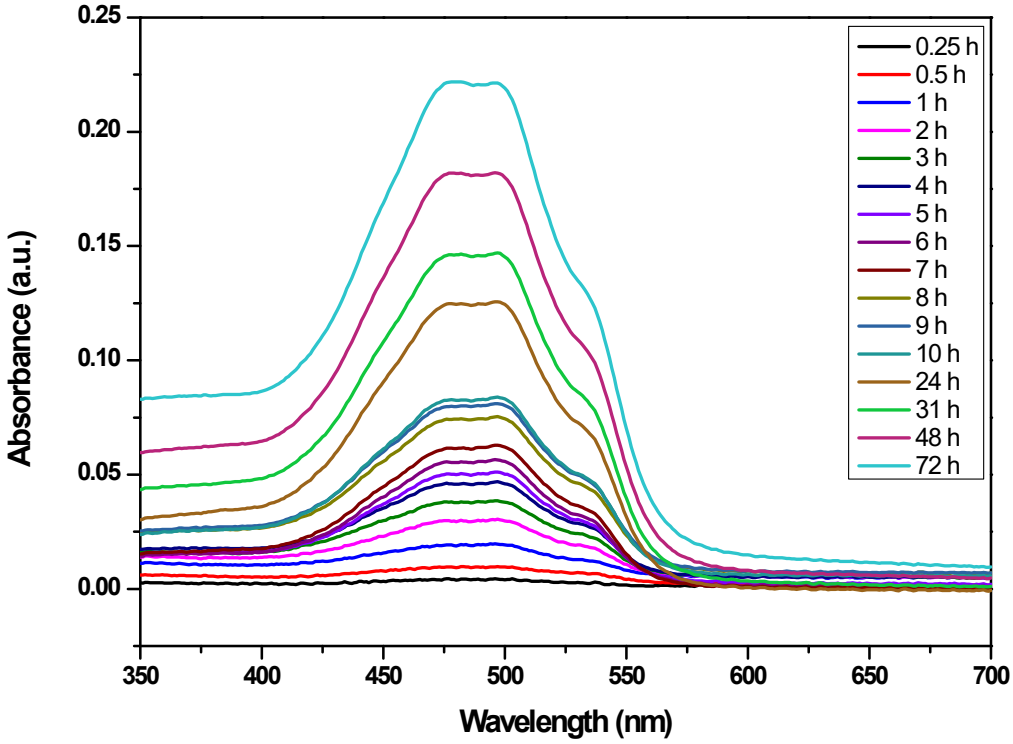

Figure S17. UV-Vis absorption spectra of DOX release form HPMO at pH 5.5 (37 °C).

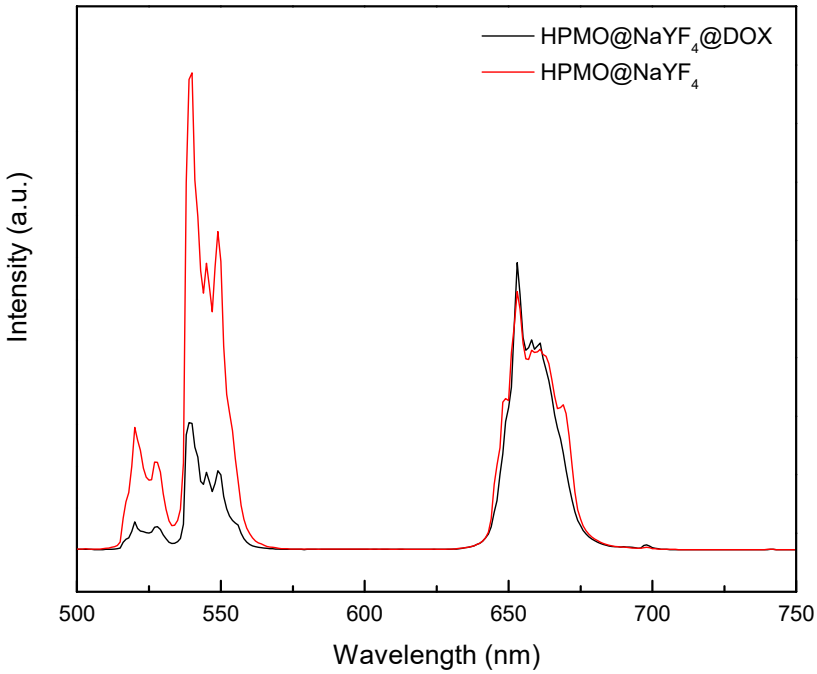

Figure S18. Emission spectrum of HPMO@$NaYF_4$:Er,Yb without and with DOX. The green emission is clearly quenched upon loading the material with DOX. The red emission is not affected by DOX.

References:

1. H. Xia, L. Lei, J. Xia, Y. Hua, D. Deng, S. Xu, *J. Lumin.*, 2019, **209**, 8.